Article

J. Biol. Regul. Homeost. Agents. 2024; 38(8): 5699–5710
https://doi.org/10.23812/j.biol.regul.homeost.agents.20243808.457

IL18 is a Prospective Target Affecting Radioiodine Therapy Sensitivity and Prognosis in Differentiated Thyroid Carcinoma

Jing Li[1], Xiaoxiang Qin[1], Junhong Li[1], Qiteng Lu[1], Zhixiao Wei[1,*]

[1]Department of Nuclear Medicine, The First Affiliated Hospital of Guangxi Medical University, 530021 Nanning, Guangxi, China
*Correspondence: weizhixiao196493@126.com (Zhixiao Wei)
Submitted: 1 February 2024 Revised: 14 March 2024 Accepted: 26 March 2024 Published: 1 August 2024

Background: Differentiated Thyroid Carcinoma (DTC) presents diverse patient outcomes, highlighting the need to identify reliable prognostic biomarkers. This study focuses on the role of interleukins, particularly interleukin18 (*IL18*), in predicting survival rates and treatment responses among DTC patients.

Methods: We conducted a comprehensive analysis of the association between various pyroptosis-related genes (*IL18*, *IL1A*, *IL6*, Granzyme A (*GZMA*), and Neutrophil elastase (*ELANE*)) and overall survival in DTC. The study employed univariate and multivariate Cox models to assess the prognostic value of these cytokines. Additionally, a nomogram model was created, integrating clinical characteristics to improve the precision of predicting patient outcomes. *IL18* expression levels in DTC tissues compared to normal tissues were examined, along with their association with patient survival and response to radioactive iodine (RAI) therapy.

Results: *IL18* emerged as a significant protective factor associated with better survival outcomes, exhibiting higher expression levels in DTC tissues compared to normal tissues. However, its expression was notably lower in RAI-refractory or high-risk groups. This study also identified axitinib as a potential therapeutic agent for high-risk DTC cases, supported by drug prediction analysis. Furthermore, immune cell analysis linked high *IL18* expression with an abundance of specific T cells, indicating its involvement in regulating the immune response and influencing the effectiveness of RAI treatment.

Conclusions: *IL18* holds promise as a prognostic biomarker in DTC, offering valuable insights into patient survival and potential treatment pathways. This study emphasizes the importance of combining molecular and clinical data to improve prognostic models and therapeutic strategies, highlighting the need for further research into the mechanisms of action of *IL18* in DTC.

Keywords: *IL18*; thyroid neoplasms; survival analysis; iodine; molecular docking simulation

Introduction

Differentiated Thyroid Carcinoma (DTC) is the most common subtype of thyroid carcinoma, with a favorable prognosis in most cases. The 10-year survival rate exceeds 95% [1–3], and about 85% of cases are curable through surgery and radioactive iodine (RAI) therapy [4]. However, a striking 60% of patients with aggressive metastatic DTC developed resistance to RAI treatment, resulting in a poor overall prognosis. Patients with DTC refractory to RAI therapy have a notably low 10-year survival rate of only 10% following metastasis [4,5]. A study shows that patients with RAI-refractory DTC have a life expectancy of less than five years [6]. RAI refractoriness is characterized by a loss of thyroid differentiation features, such as the impaired function of the Na/I symporter (NIS), crucial for iodine concentration in follicular cells used in RAI therapy [7]. Despite this, the exact molecular mechanism behind RAI-refractory DTC remains incompletely understood, and effective therapeutic strategies are currently lacking. Prolonging the life expectancy of patients with RAI-refractory DTC poses a significant challenge for clinicians. Hence, there is an urgent need to explore new treatment targets for RAI refractory DTC. In this study, we aim to determine the underlying gene responsible for the limited curative efficacy of RAI-resistant DTC. Given that pyroptosis is associated with inflammatory and immune responses in many types of cancers [8,9], we sought to investigate its potential in DTC. It has been documented that prolonged exposure to an inflammatory environment increases the likelihood of cellular and tissue oncogenesis. Particularly, the release of cytokines elicited by pyroptosis, including interleukin 1 (*IL1*) and *IL18*, can promote tumor infiltration, consequently augmenting the probability of tumorigenesis and metastasis [10]. After analyzing the transcriptome data of DTC from both Gene Expression Omnibus (GEO) and The Cancer Genome Atlas (TCGA) databases, we noticed that the lower expression of a pyroptosis-related gene—*IL18*—might be linked to RAI resistance and poor outcomes in DTC. This reduced expression could be responsible for the

Journal of
BIOLOGICAL REGULATORS
and Homeostatic Agents

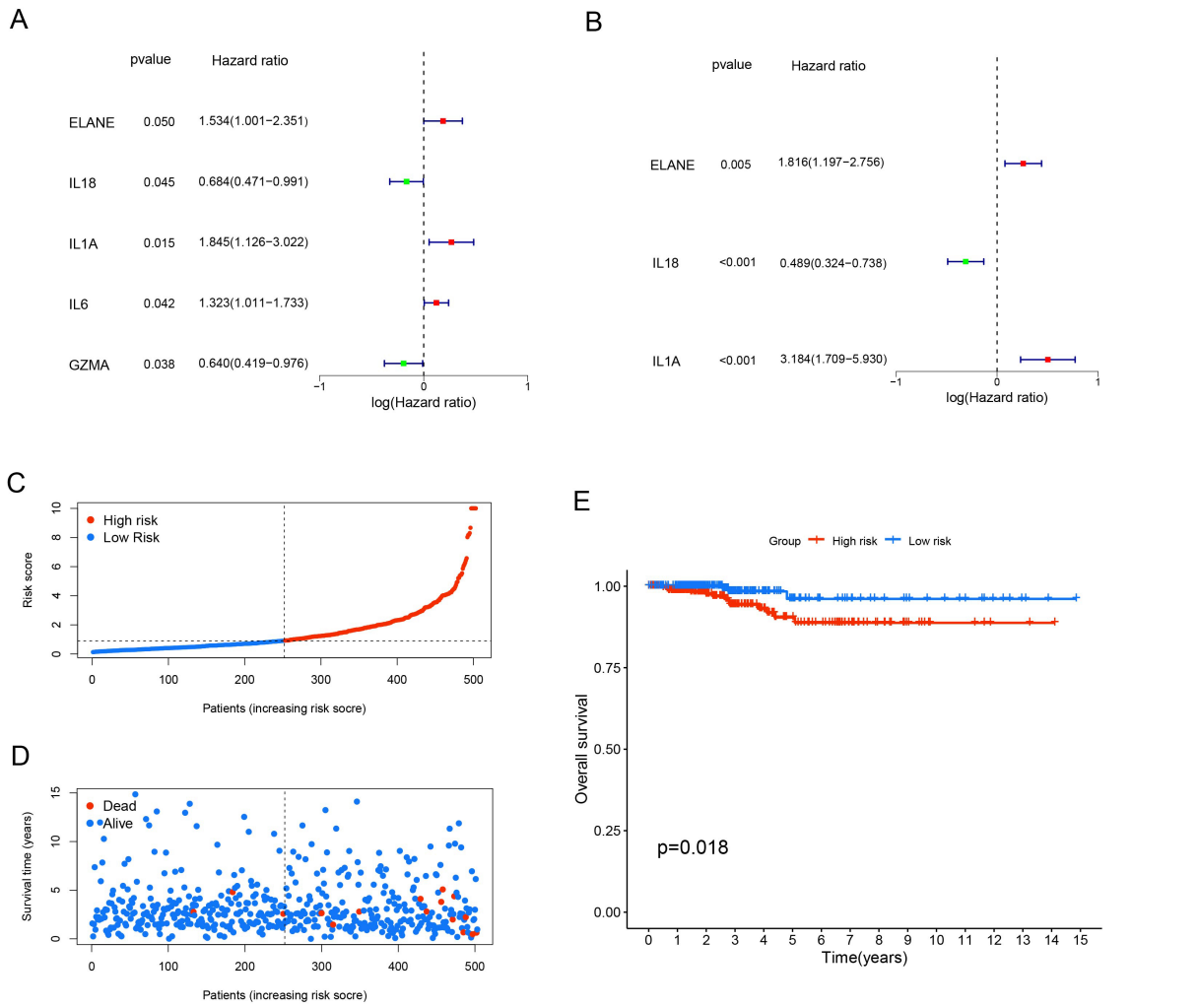

Fig. 1. Risk mRNAs screening and risk mRNAs model construction. (A) Significant genes in the univariate Cox model. The green bar at the left side of the forest plot is a protective gene. The red bar at the right side of the forest plot is a risk factor. (B) Significant genes in the multivariate Cox model. (C,D) Risk curve and survival state diagram of DTC in The Cancer Genome Atlas (TCGA). (E) The K-M curves of the high-risk and low-risk groups. *ELANE*, Neutrophil elastase; *IL*, interleukin; *GZMA*, Granzyme A; DTC, Differentiated Thyroid Carcinoma; K-M, Kaplan-Meier.

lower presence of immune cells like follicular helper T cells and CD4 memory-activated T cells, which are crucial for tumor surveillance and immunity. Finally, we identified several potential small drugs for treating DTC with a poor prognosis through molecular docking methods. Our study sheds light on a new mechanism for RAI-resistant DTC and provides promising drug targets related to this mechanism. This work introduces a new avenue for addressing the challenge of RAI resistance in DTC and could significantly benefit future research.

Materials and Methods

Data Preparation

Microarray dataset GSE151170 of DTC, containing four avid and 48 refractory samples after treatment with RAI, was downloaded from the GEO database. Data for 570 thyroid carcinoma cases were downloaded from the TCGA database, of which 503 DTC cases contain both clinical and expression data.

Prognostic Model Construction

A total of 52 pyroptosis-related genes, including *IL18*, *IL1A*, *IL6*, Granzyme A (*GZMA*), and Neutrophil elastase (*ELANE*), were identified through text mining. Univariate Cox analysis was performed on the TCGA dataset using the survival package (3.2-13) in R software (https://cloud.r-project.org/bin/windows/base/old/4.1.2/) based on these genes. Subsequently, a multivariate Cox model was employed using a stepwise procedure in both directions to further evaluate the significant features identified in the univariate analysis. The significant genes in the multivariate Cox model were designated as risk mRNAs, and the model itself was referred to as the risk mRNAs model.

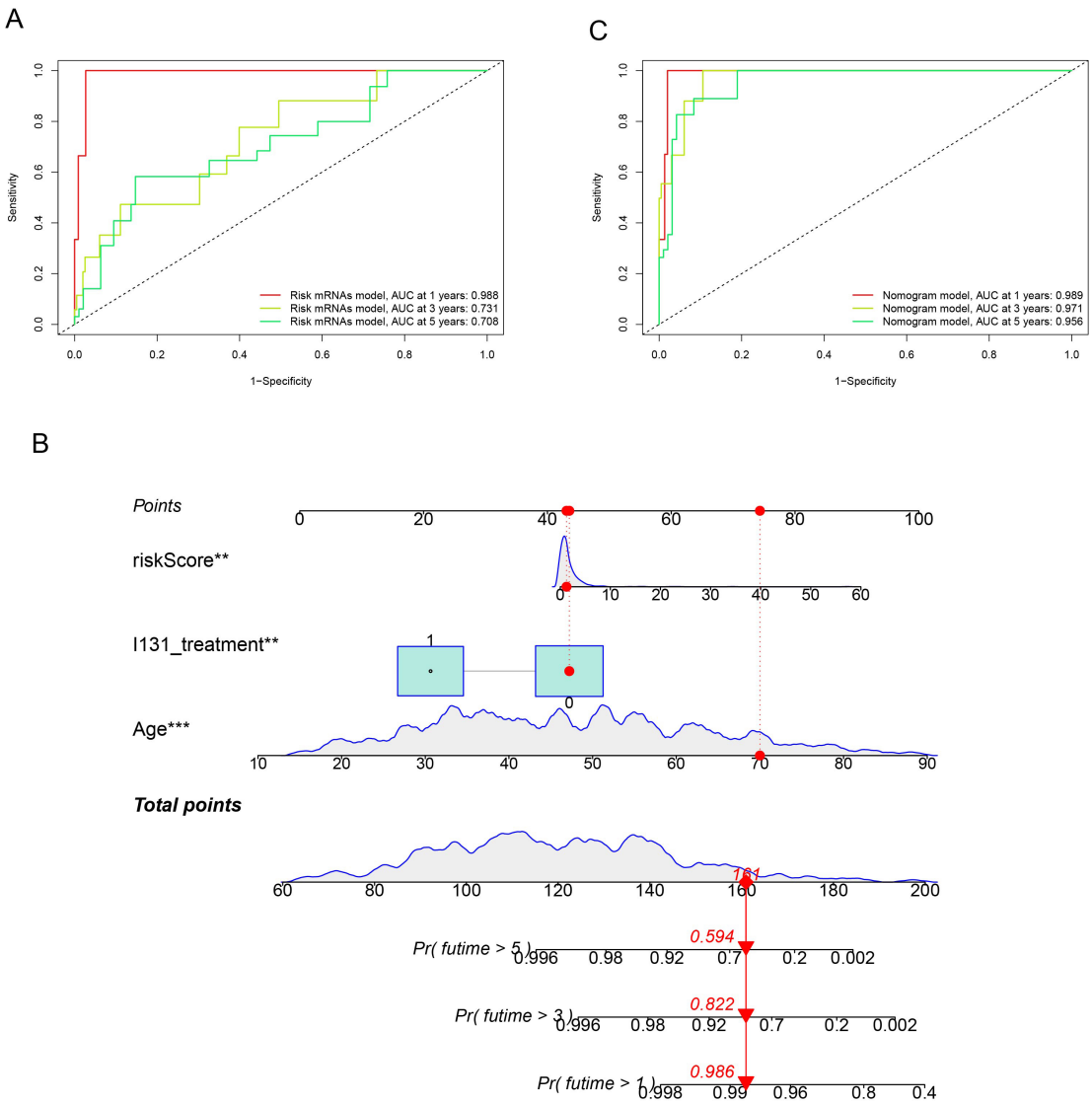

Fig. 2. Prognostic model construction and diagnostic ability determination. (A) The ROC curve for the first, third, and fifth years of the risk mRNA model. (B) The nomogram diagram of the nomogram model. (C) The ROC curve for the first, third, and fifth years of the nomogram model. ROC, receiver operating characteristic. Statistically significant variables, $^{**}p < 0.01$, $^{***}p < 0.001$.

The risk scores for each sample were calculated using the risk mRNA model according to the formula: $Riskscore = h_0(t) \times exp\,(\beta_1 X_1 + \beta_2 X_2 + ... + \beta_n X_n)$. In this equation, X_1 to X_n represent genes significantly expressed in the multivariate Cox model, while β_1 to β_n were the coefficients of these significant genes. The 503 DTC cases were then divided into two groups based on their risk scores: those with scores below the median were classified as the low-risk group, and those above as the high-risk group. Survival analyses were conducted using Kaplan-Meier (K-M) methods, and a long-rank test was employed to determine the significance between the high-risk and low-risk groups. A nomogram model was developed using the risk scores generated from the mRNA risk model and three key clinical characteristics: age, gender, and RAI treatment.

Gene Differential Expression Analysis

Microarray Data Analysis of DTC from the GEO Database

After removing probes matching several genes, the average expression value was calculated using probes specific to individual genes. Subsequently, we conducted a differentially expressed genes (DEGs) analysis between the avid and refractory groups of RAI therapy. This analysis was performed using the limma package (3.50.0) [11]. Differentially expressed genes were identified based on a significance criterion of p-value < 0.05 and log2 fold change (log FC) >1.

Sequencing Data Analysis of DTC from the TCGA Database

For the sequencing data of DTC from the TCGA database, DEGs analysis was performed using the DESeq2

Journal of
BIOLOGICAL REGULATORS
and Homeostatic Agents

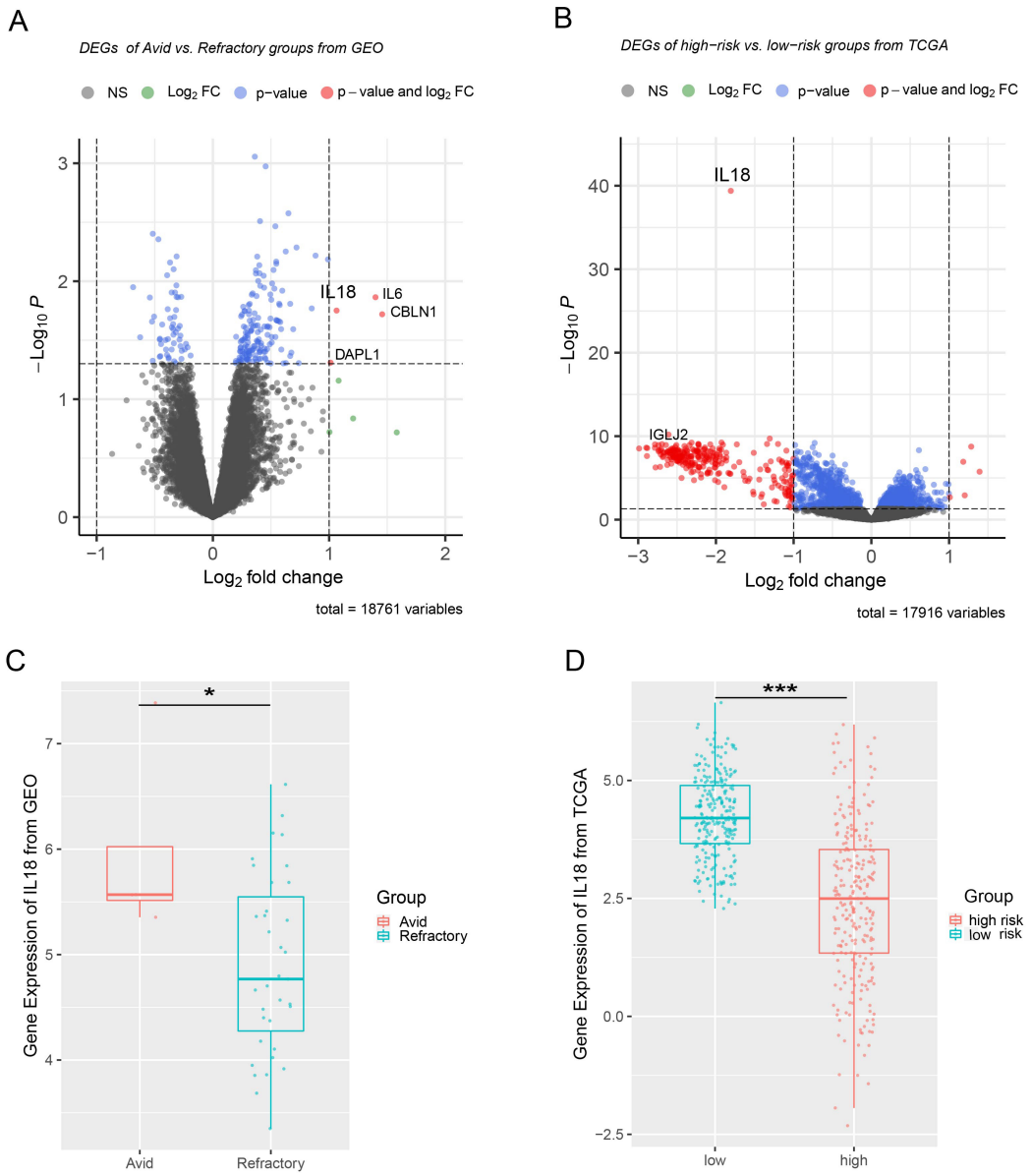

Fig. 3. Comparison of the *IL18* expression between different types of groups. (A) The volcano plot of DEGs between the avid and refractory groups of DTC from the DEO database. (B) The volcano plot of DEGs between the high-risk and low-risk groups of DTC from the TCGA database. (C) *IL18* expression between the avid group and the refractory group (*$p < 0.05$). (D) *IL18* expression between the high-risk and low-risk groups (***$p < 0.001$). DEGs, differentially expressed genes; GEO, Gene Expression Omnibus.

package (https://bioconductor.org/packages/release/bioc/html/DESeq2.html) [12]. Differentially expressed genes were determined with an adjusted p-value < 0.01 and logFC >1.5.

IL18 Expression in Normal Tissue and Thyroid Carcinoma

We explored the expression of *IL18* using the TCGA TARGET GETx study available on the UCSC Xena database. The study addressed batch effects caused by different computational processing by re-analyzing samples from TCGA, TARGET, and GTEx using a consistent RNA-seq workflow. The gene expression dataset utilized was "RSEM expected_count (DESeq2 standardized)", normalized through the DESeq2 method. A Welch's t-test was used to compare *IL18* expression levels between normal tissue from GETx and thyroid carcinoma from TCGA. Additionally, the Human Protein Atlas (HPA) database (https://www.proteinatlas.org/) provided insights into *IL18* expression at the protein level, serving as a verification method [13].

Tumor Immune Evasion Analysis

The Tumor Immune Dysfunction and Exclusion (TIDE) database (http://tide.dfci.harvard.edu/login/) was utilized to assess the potential of tumor immune evasion.

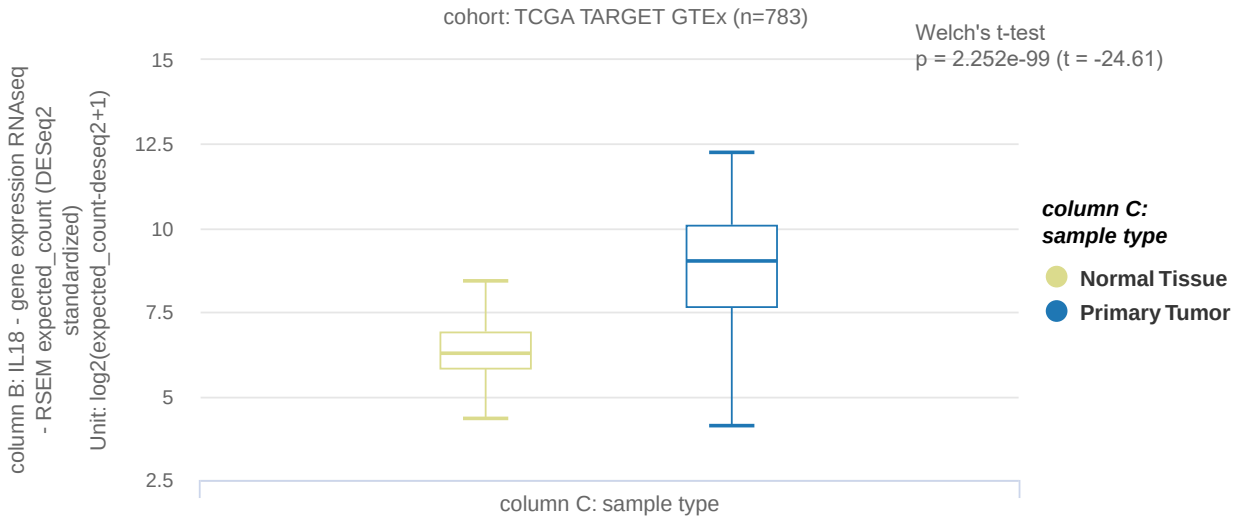

Fig. 4. *IL18* expression from normal tissue and primary tumor of the thyroid gland.

A higher TIDE score indicates an increased likelihood of tumor immune evasion and suggests a reduced benefit from immune checkpoint blockade therapy. To compare the TIDE scores between the two groups, two-sample Wilcoxon tests were used.

Identification of Immune Cells Associated with IL18 in DTC

We assessed the abundance of different immunocytes in DTC samples from TCGA using the CIBERSORT package (version 1.03, SU, Stanford, CA, USA) [14]. Subsequently, we identified the immune cell types associated with *IL18* expression levels using the Spearman method.

Prediction of Potential Chemotherapy Drugs for High-Risk DTC

The chemotherapeutic drug sensitivity of high-risk and low-risk groups was evaluated using the pRRophetic package (https://github.com/paulgeeleher/pRRophetic) [15]. Two-sample Wilcoxon tests were used to compare drug sensitivity (Half Maximal Inhibitory Concentration, IC50) between the high-risk and low-risk groups. Additionally, a correlation test between drug sensitivity and risk scores was performed using the Spearman rank correlation test. Drugs with a p-value $< 1 \times 10^{-3}$ in two-sample Wilcoxon tests and a coefficient <–0.2, and p-value $< 1 \times 10^{-5}$ in the Spearman rank correlation test were identified as potential candidate drugs for high-risk DTC. A correlation coefficient <–0.2 indicated higher drug sensitivity in the high-risk group compared to the low-risk group. Molecular docking studies were performed using AotoDock Vina software (https://vina.scripps.edu/) to analyze interactions between candidate drugs and *IL18* [16]. The 2D structures of the candidate drugs were downloaded from the PubChem database (https://pubchem.ncbi.nlm.nih.gov/), while the crystal structure of *IL18* was retrieved from the Protein Data Bank (PDB) database. Successful docking is achieved when the root-mean-square deviation (RMSD) of the ligand is less than 1 Å relative to the initial crystal structure, and the docking affinity is below –0.6 kcal/mol. The docking results were visualized using PyMOL software (https://pymol.org/). Protein-ligand interaction analysis was performed using the PLIP web tool (https://plip-tool.biotec.tu-dresden.de/plip-web/plip/index) [17].

Statistical Analysis

Student's t-test was used to compare two independent groups with data following a normal distribution. In cases where the data did not exhibit a normal distribution, the Wilcoxon rank sum test was employed for comparison. Welch's t-test was specifically applied for two-sample comparisons within the TCGA TARGET GETx study. The Spearman rank correlation test was utilized to evaluate correlations between two quantitative variables. Univariate and multivariate analyses were conducted using the Cox proportional hazard regression model. Survival curves generated through the K-M method were compared using the log-rank test. Statistical significance was determined at $p < 0.05$.

Results

Risk mRNAs Screening and Risk mRNAs Model Construction

ELANE, *IL18*, *IL1A*, *IL6*, and *GZMA* were significantly associated with overall survival in the univariate Cox models (Fig. 1A). In the multivariate Cox model, *IL18*, *ELANE*, and *IL1A* emerged as independent predictors of overall survival through both forward and backward stepwise regression (Fig. 1B). Among these, *IL18* was identi-

Journal of
BIOLOGICAL REGULATORS
and Homeostatic Agents

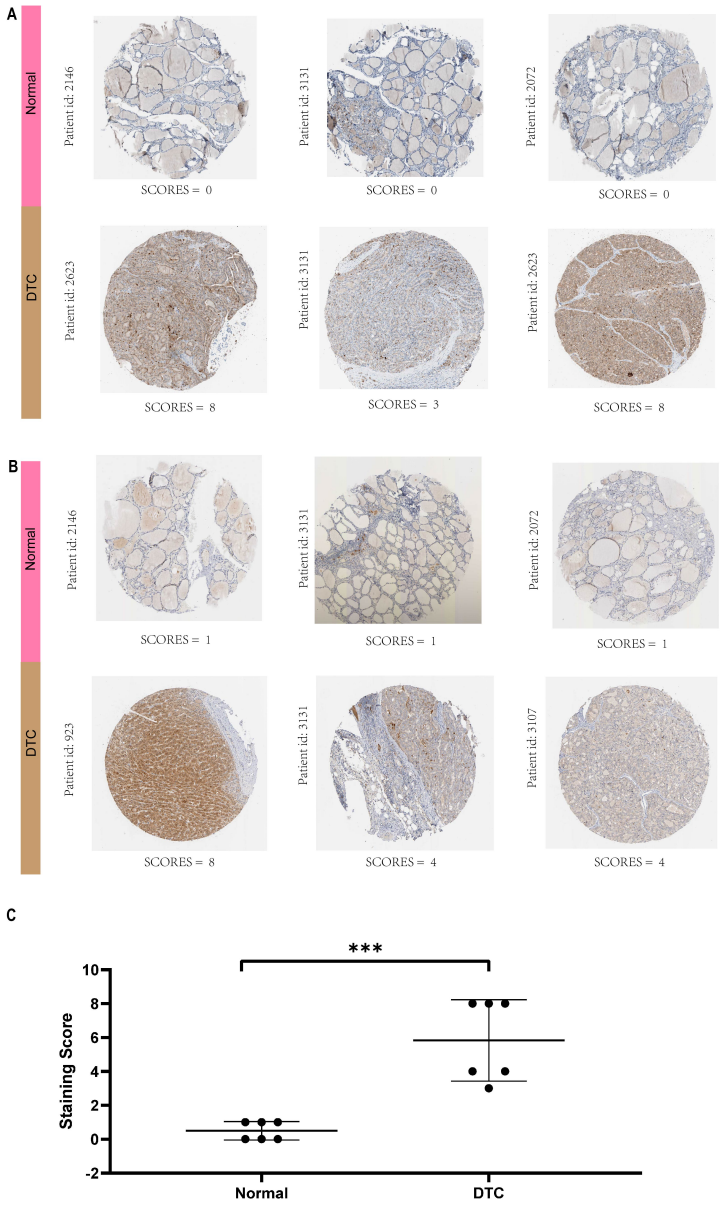

Fig. 5. Protein expression of *IL18* in normal tissue and DTC sample. (A) Protein detected with the antibody HPA003980. (B) Protein detected with the antibody CAB007772. (C) *IL18* expression in normal and DTC tissues, as determined by combined results from immunohistochemical studies using the antibodies HPA003980 and CAB007772 (***$p < 0.001$). HPA, Human Protein Atlas.

fied as a protective factor, while *ELANE* and *IL1A* were considered risk factors. The risk score, calculated using the formula $5.316 \times \exp(0.597 \times ELANE - 0.715 \times IL18 + 1.158 \times IL1A)$, was determined to be 0.911. Based on this definition, individuals with a risk score exceeding 0.911 were placed in the high-risk group (251 cases), whereas those below 0.911 were assigned to the low-risk group (252 cases) (Fig. 1C). Among the total cases, 487 cases were alive, while 16 were dead (Fig. 1D). The K-M survival analysis revealed that the low-risk group had a significantly longer average survival time compared to the high-risk group (14.43097 $\pm$ 0.2646299 *vs* 13.54635 $\pm$ 0.365017, unit = year, $p = 0.018$) (Fig. 1E). This indicates that individuals in the high-risk group are more likely to experience poorer outcomes than those in the low-risk group.

Prognostic Model Construction and Diagnostic Ability Determination

The receiver operating characteristic (ROC) curves for the risk mRNAs model's first, third, and fifth years are displayed in Fig. 2A. In Fig. 2B, it is evident that the area under the ROC curve (AUC) exceeded 90% in the first year but declined significantly thereafter, dropping below 80% in the third and fifth years. While the risk mRNA model demonstrates strong short-term diagnostic efficacy, its long-term diagnostic ability is poor. To address this,

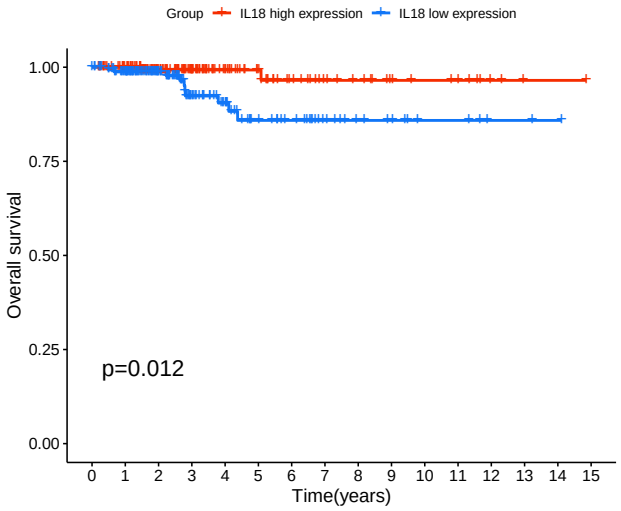

Fig. 6. Survival analysis between the *IL18* low expression group and *IL18* high expression group on the gene expression RNAseq data of the HPA database.

a nomogram model was developed incorporating the risk score from the mRNA model along with clinical factors such as age and I131 treatment history, while RAI treatment history acts as a protective factor (Fig. 2B). As shown in Fig. 2C, all AUC values for the first, third, and fifth years are more than 90%, indicating improved diagnostic stability of the new model compared to the previous model (Fig. 2C).

Comparison of the IL18 Expression between Different Types of Groups

IL18 is significantly expressed in both the GEO and TACGA datasets of DTC (Fig. 3A,B). Notably, the expression of *IL18* was markedly higher in avid groups compared to RAI-refractory groups ($p < 0.05$) (Fig. 3C). Furthermore, the expression of *IL18* demonstrated a substantial increase in the low-risk group compared to the high-risk group ($p < 0.001$) (Fig. 3D). It is noteworthy that both the RAI-refractory and high-risk groups exhibited higher levels of *IL18* compared to their counterparts. These findings suggest a shared characteristic between these two groups that potentially leads to the downregulation of *IL18* expression.

Thyroid Carcinoma has a Significantly Higher Level of IL18 Expression than Healthy Tissue

The significant differences in *IL18* expression between normal thyroid tissue and primary thyroid carcinoma were examined using Welch's *t*-test. Notably, the expression of *IL18* was significantly higher in the primary tumor group compared to the normal tissue group ($p < 0.001$) (Fig. 4). This result was further verified by analyzing the protein expression of *IL18* in the HPA database. The staining score was calculated by multiplying the intensity score with the quantity score obtained from the immunohistochemical section [18]. Intensity levels were categorized as negative, weak, moderate, or strong, corresponding to scores of 0, 1, 2, and 3, respectively. Similarly, quantity levels were rated into four levels: none, (0%–25%], (25%–50%], (50%–75%], or (75%–100%] and were given a score of 0, 1, 2, 3, or 4, accordingly. Protein expression of *IL18* was detected using the antibodies HPA003980 (Fig. 5A) and CAB007772 (Fig. 5B). In Fig. 5A,B, the staining sores for the DTC group were notably higher than those for the normal group, regardless of whether detected by the antibody HPA003980 or CAB007772. As shown in Fig. 5C, the protein expression of *IL18* was significantly higher in DTC tissue compared to normal tissue. A survival analysis conducted using the gene expression RNAseq data (DESeq2 standardized) from the HPA database revealed that the group with high *IL18* expression had significantly longer survival time than the group with low *IL18* expression ($p < 0.05$) (Fig. 6).

Table 1. Docking results between *IL18* and the candidate drugs.

Docking receptor	Candidate drugs	Docking affinity	RMSD
IL18	Axitinib	–6.7	0
IL18	Elesclomol	–6.8	1.521
IL18	Fedratinib	–6.4	2.799

RMSD, root-mean-square deviation.

Prediction of Tumor Immune Evasion Capacity

The analysis of tumor immune evasion revealed significantly higher TIDE scores in the RAI-refractory group compared to the avid group ($p < 0.01$) (Fig. 7A). Conversely, the high-risk group exhibited higher TIDE scores than the low-risk group ($p < 0.001$) (Fig. 7B). These results suggest that both the RAI-refractory and high-risk groups have a higher tumor evasion capacity.

Immune Cells Associated with IL18 Expression in DTC

Fig. 8A illustrates a notable correlation between the abundance of follicular helper T cells, CD4 memory-activated T cells, and the expression of *IL18* in DTC tissue. Furthermore, in DTC samples, the abundance of follicular helper T cells and CD4 memory-activated T cells showed a negative correlation with risk scores, with *p*-values of 0.014 and 0.0027, respectively (Fig. 8B,C). These findings indicate a potential explanation for the lower *IL18* expression in the high-risk group compared to the low-risk group.

Potential Drug Prediction and Verification

We identified three potential drugs for the treatment of DTC. The drug sensitivity (IC50) of these candidate drugs showed a negative correlation with the corresponding risk score, with all *p*-values < 0.001 according to Spearman's rank correlation coefficient (Fig. 9A). Furthermore, the drug sensitivity was significantly higher in the high-risk

Journal of
BIOLOGICAL REGULATORS
and Homeostatic Agents

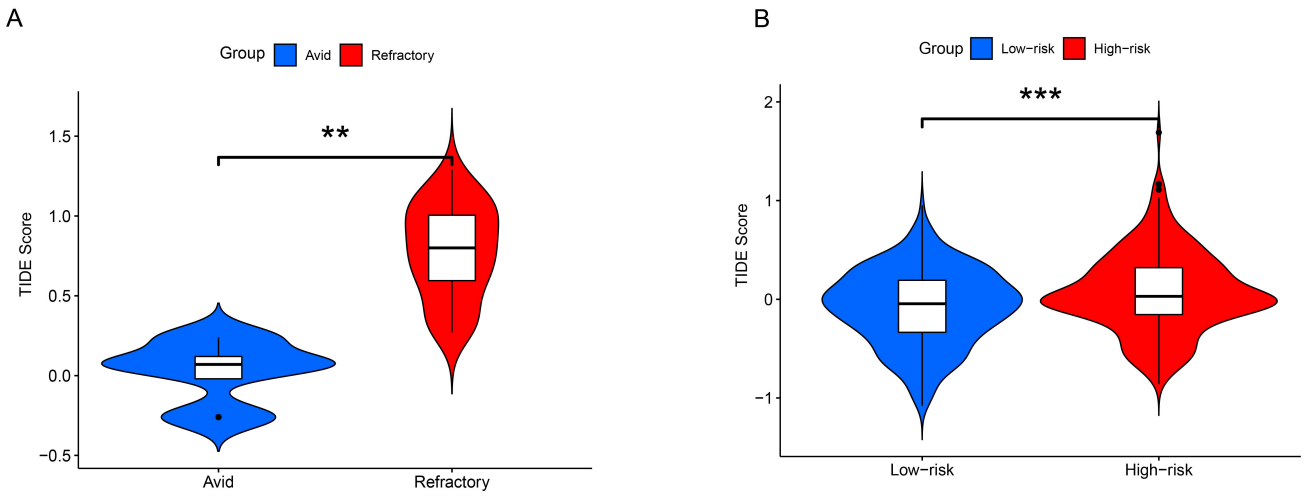

Fig. 7. Prediction of tumor immune evasion capacity. (A) TIDE scores between the avid group and the refractory group (**$p < 0.01$). (B) TIDE scores between the low-risk-group and high-risk group (***$p < 0.001$). TIDE, Tumor Immune Dysfunction and Exclusion.

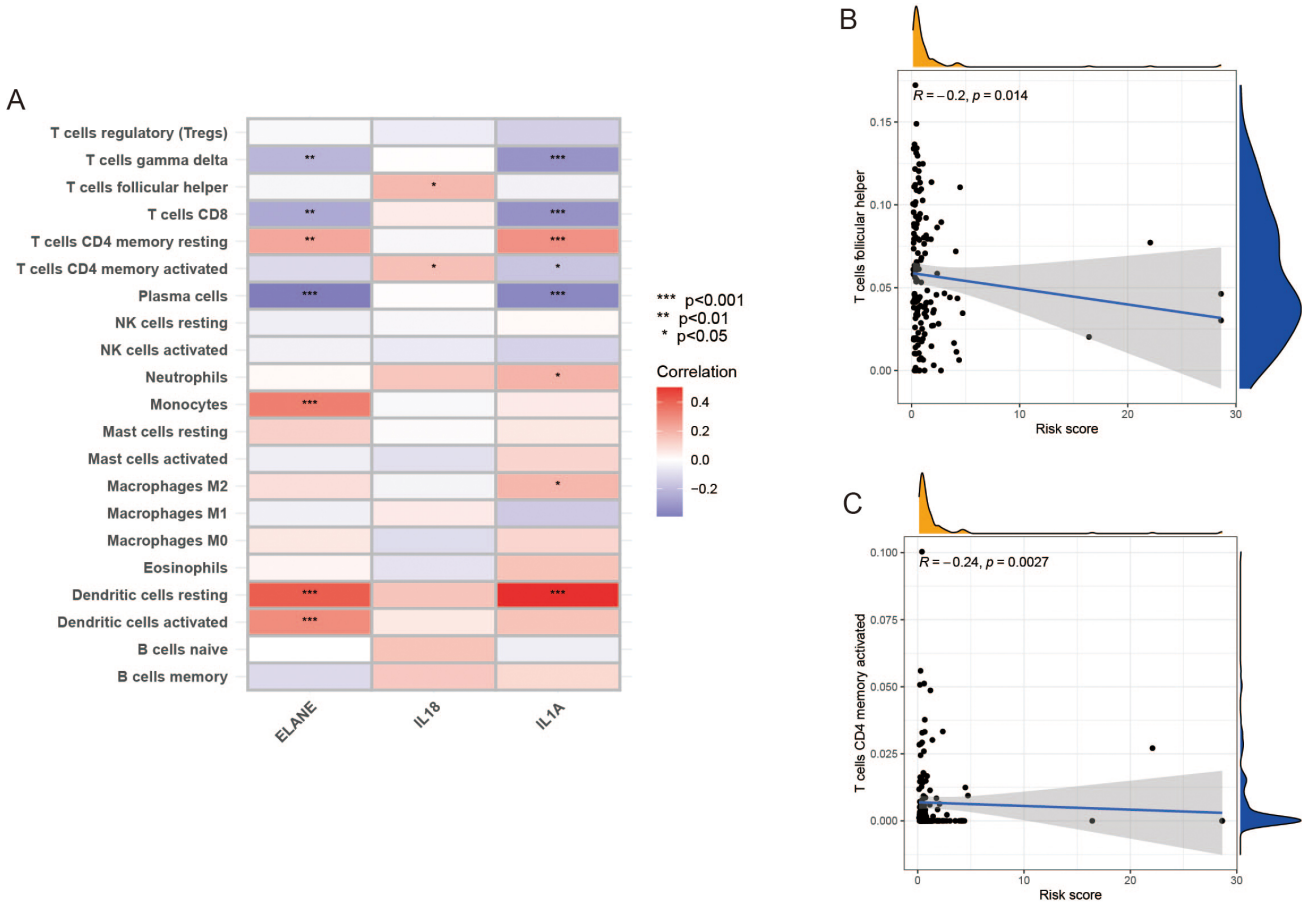

Fig. 8. Association of immune cells with the expression of risk genes. (A) Association between immune cells abundance and the expression of risk genes. (B) Association between the abundance of follicular helper T cells and risk scores in DTC samples. (C) Association between CD4 memory activated T cells and risk scores in DTC samples.

group compared to the low-risk group, with all p-values < 0.001 based on the Wilcoxon rank sum test (Fig. 9B). These findings suggest that these candidate drugs may be effective against the high-risk group of DTC in the IC50 level.

Among these small drugs, only axitinib meets the criteria of RMSD values ≤1 Å and docking affinity values ≤–6.0 kcal/mol when docked with *IL18* (Table 1). Fig. 10 shows the specific docking sites between the small drugs and *IL18*.

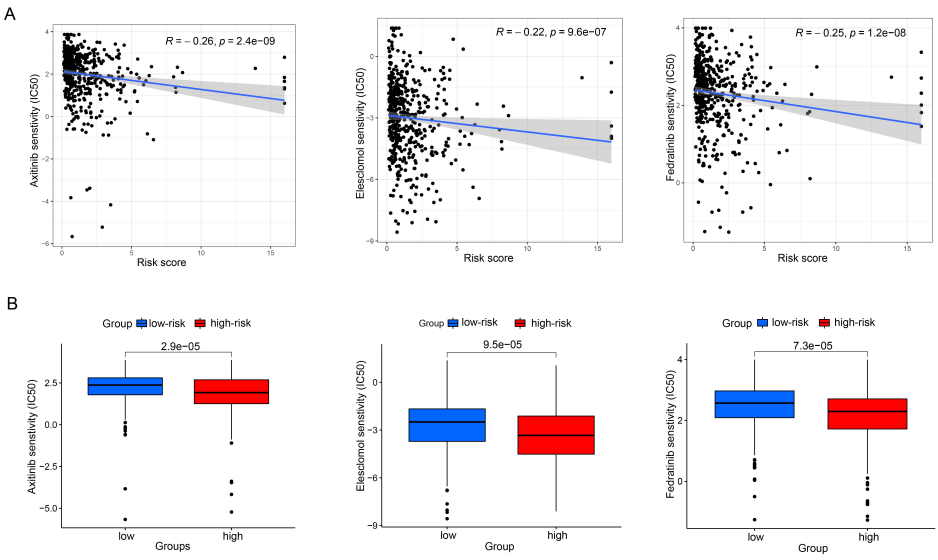

Fig. 9. Drug prediction and verification. (A) The scatter plots between drug sensitivity (IC50) and the risk scores. (B) Comparison of drug sensitivity (IC50) between the high-risk and low-risk groups. RMSD, root-mean-square deviation; IC50, Half Maximal Inhibitory Concentration.

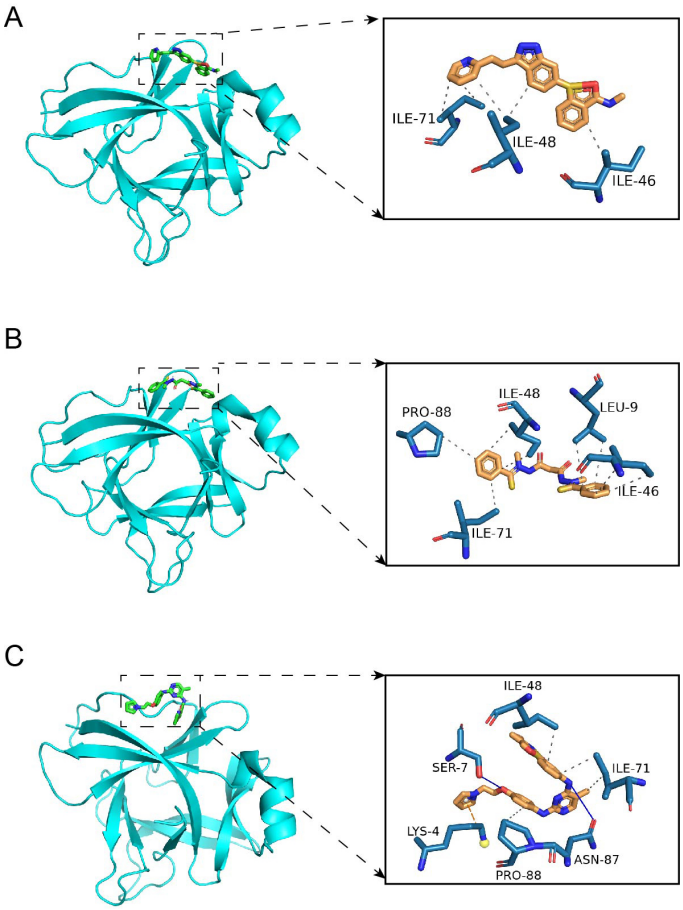

Fig. 10. Representation of the specific docking sites between the small drugs and *IL18*. Docking results between *IL18* with Axitinib (A), Elesclomol (B), and Fedratinib (C), respectively. Explanation about the characters in the black box: The light blue bar is the amino acid residue in *IL18*. The yellow bar is the drugs that bind to *IL18*. The solid line is a hydrogen bond. The dotted line is hydrophobic interaction. The yellow ball is the charge center. The white ball is the aromatic ring center.

Journal of
BIOLOGICAL REGULATORS
and Homeostatic Agents

Discussion

The findings from this study highlight the significant association between specific interleukins (*IL18*, *IL1A*, *IL6*, *GZMA*, and *ELANE*) and overall survival in Differentiated Thyroid Carcinoma (DTC), underscoring their potential as prognostic biomarkers. Notably, *IL18* emerged as a protective factor. While a prognostic model based on these markers demonstrated solid short-term diagnostic efficacy, its long-term predictive ability was limited. To address this limitation, clinical attributes were integrated into a nomogram model, improving diagnostic reliability. Additionally, *IL18* expression was significantly higher in DTC tissues compared to normal tissues and was associated with improved survival rates. The study also explored tumor immune evasion, showing higher TIDE scores in RAI-refractory and high-risk groups, indicating greater tumor immune evasion capacity. Immune cell analysis linked *IL18* expression to specific T cell abundance, suggesting a role in modulating immune responses. Finally, drug prediction analysis identified axitinib as a potential therapeutic agent for high-risk DTC cases. This comprehensive analysis underscores the complexity of DTC prognosis and the potential of integrating molecular and clinical data for improved prediction models. The outcomes of patients with DTC differ dramatically depending on their response to RAI treatment [19], whether resistant or responsive. A poor outcome may result from resistance to RAI therapy. Our findings revealed that the RAI-refractory group exhibited significantly lower levels of *IL18* expression compared to the RAI-avid group. These findings suggest that *IL18* expression could influence the response of DTC to RAI therapy. Conversely, the expression of *IL18* was relatively lower in the high-risk group than in the low-risk group, indicating that certain endogenous or exogenous characteristics of high-risk DTC may contribute to a lower expression of *IL18*.

IL18, a crucial pro-inflammatory cytokine and effector molecule of pyroptosis and carcinoma, has been the focus of studies [20–22]. However, few studies have explored its role in DTC. Our analysis of *IL18* expression in the TCGA TARGET GTEx project revealed significantly higher levels in primary thyroid tumor compared to normal thyroid tissue. This result is in line with the protein expression data from the HPA database. Moreover, the high-expression group of *IL18* exhibited a notably higher survival rate than the low-expression group. This observation is consistent with previous survival analyses comparing *IL18* DEGs in low-risk and high-risk groups. These results underscore the potential of *IL18* as a crucial prognostic factor in determining outcomes for patients with DTC. Several prior studies have discovered that polymorphisms of *IL18* might increase susceptibility to thyroid cancer [23,24], suggesting a role for *IL18* in the outcome of DTC. However, the mechanism of *IL18* expression in different subtypes of DTC remains unclear. Fig. 3C,D show that high levels of *IL18* are linked to better outcomes for patients. *IL18*, as an inflammatory cytokine, is naturally found in higher concentrations in tumor tissues than in normal tissues, as confirmed by the data in Figs. 4,5. Interestingly, *IL18* levels are higher in patients with low-risk DTC compared to those at higher risk, indicating a potentially weaker immune in high-risk patients. This difference could stem from high-risk tumors' enhanced ability to evade the immune system or from the reduced effectiveness of lymphocytes in launching a strong immune response. A similar concept is observed in tuberculosis patients with the Purified Protein Derivative (PPD) test, where a stronger reaction usually indicates a robust immune system [25]. Similarly, higher *IL18* levels in DTC may indicate a more robust immune response, often associated with a favorable prognosis. Our research revealed a significant association between the abundance of follicular helper T cells and CD4 memory-activated T cells and the expression of *IL18* in DTC tissue. Furthermore, the abundance of these cells exhibits a negative correlation with the risk scores observed in DTC samples. These findings provide a potential rationale for the reduced expression of *IL18* in the high-risk group.

The analysis of tumor immune evasion revealed that both the RAI-refractory and the high-risk groups exhibit higher TIDE scores compared to their counterparts, indicating superior immune evasion capabilities. Three potential drugs have been identified for the treatment of high-risk DTC: Axitinib, Elesclomol, and Fedratinib. These drugs demonstrate lower IC50 values in the high-risk group than in the low-risk group, potentially offering therapeutic benefits for high-risk DTC. Among these candidate drugs, only Axitinib successfully docked with *IL18* based on specific criteria (docking affinity $\leq$–6.0 kcal/mol and RMSD $\leq$1.0 Å). Study has demonstrated the significant impact of vascular endothelial growth factor (VEGF) and its receptor (VEGFR) on thyroid cancer development [26]. Axitinib, a potent and selective VEGFR inhibitor, has shown promising therapeutic efficacy in clinical trials for treating RAI-resistant DTC [27,28].

Our study sheds light on the significance of *IL18* expression in the prognosis of DTC, recognizing the inherent limitations of retrospective analyses. It is crucial to conduct prospective studies to validate these findings and further elucidate the molecular mechanisms of *IL18*'s role in DTC. Future research should focus on unraveling the molecular interactions and pathways that underlie the prognostic implications of *IL18* and other related genes, paving the way for novel therapeutic strategies and enhanced prognostic models for DTC.

Conclusions

This study underscores the significance of *IL18* as a potential prognostic biomarker in DTC, demonstrating its

protective role in patient outcomes. *IL18* expression was notably higher in DTC tissues compared to normal thyroid tissues, but lower in the refractory or high-risk DTC group, correlating with improved survival rates. This correlation suggests *IL18*'s pivotal role in modulating immune responses and potentially influencing the effectiveness of treatments, such as RAI therapy. These findings support further investigation into *IL18* mechanisms of action within DTC, emphasizing its importance in developing more precise prognostic models and targeted therapeutic strategies.

Availability of Data and Materials

All experimental data included in this study are available upon request by contacting the first author. Alternatively, the data can be downloaded from the following databases: GEO: https://www.ncbi.nlm.nih.gov/geo/; TCGA: https://portal.gdc.cancer.gov/; TCGA TARGET GETx study: https://xena.ucsc.edu/; Human Protein Atlas: https://www.proteinatlas.org/; RCSB Protein Data Bank (RCSB PDB): https://www.rcsb.org/; PubChem: https://pubchem.ncbi.nlm.nih.gov/.

Author Contributions

ZXW designed the study. QTL and JHL were responsible for consulting the literature and searching for data. XXQ provided assistance with data mining. JL conducted the data analysis and molecular docking work. JL drafted this manuscript. All authors contributed to important editorial changes in the manuscript. All authors read and approved the final manuscript. All authors have participated sufficiently in the work and agreed to be accountable for all aspects of the work.

Ethics Approval and Consent to Participate

Not applicable.

Acknowledgment

We are very grateful to Mr. Dai Yongfa from The Fifth Hospital of Guangxi Medical University for the data analysis support and guidance provided to the research.

Funding

Funding for this study was provided by the Open Research Fund Program of Collaborative Innovation Center for Molecular Imaging of Precision Medicine, No. 2020-MS04.

Conflict of Interest

The authors declare no conflict of interest.

References

[1] Rosenberg AJ, Liao CY, Karrison T, de Souza JA, Worden FP, Libao B, *et al*. A multicenter, open-label, randomized, phase II study of cediranib with or without lenalidomide in iodine 131-refractory differentiated thyroid cancer. Annals of Oncology. 2023; 34: 714–722.

[2] Ahn D, Lee GJ, Sohn JH. Recurrence following hemithyroidectomy in patients with low- and intermediate-risk papillary thyroid carcinoma. The British Journal of Surgery. 2020; 107: 687–694.

[3] Bray F, Ferlay J, Soerjomataram I, Siegel RL, Torre LA, Jemal A. Global cancer statistics 2018: GLOBOCAN estimates of incidence and mortality worldwide for 36 cancers in 185 countries. CA: A Cancer Journal for Clinicians. 2018; 68: 394–424.

[4] Liu Y, Wang J, Hu X, Pan Z, Xu T, Xu J, *et al*. Radioiodine therapy in advanced differentiated thyroid cancer: Resistance and overcoming strategy. Drug Resistance Updates. 2023; 68: 100939.

[5] Schlumberger M, Tahara M, Wirth LJ, Robinson B, Brose MS, Elisei R, *et al*. Lenvatinib versus placebo in radioiodine-refractory thyroid cancer. The New England Journal of Medicine. 2015; 372: 621–630.

[6] Durante C, Haddy N, Baudin E, Leboulleux S, Hartl D, Travagli JP, *et al*. Long-term outcome of 444 patients with distant metastases from papillary and follicular thyroid carcinoma: benefits and limits of radioiodine therapy. The Journal of Clinical Endocrinology and Metabolism. 2006; 91: 2892–2899.

[7] Ravera S, Reyna-Neyra A, Ferrandino G, Amzel LM, Carrasco N. The Sodium/Iodide Symporter (NIS): Molecular Physiology and Preclinical and Clinical Applications. Annual Review of Physiology. 2017; 79: 261–289.

[8] Fang Y, Tang Y, Huang B. Pyroptosis: A road to next-generation cancer immunotherapy. Seminars in Immunology. 2023; 68: 101782.

[9] Wei X, Xie F, Zhou X, Wu Y, Yan H, Liu T, *et al*. Role of pyroptosis in inflammation and cancer. Cellular & Molecular Immunology. 2022; 19: 971–992.

[10] Balkwill F, Mantovani A. Inflammation and cancer: back to Virchow? Lancet. 2001; 357: 539–545.

[11] Smyth GK. Linear models and empirical bayes methods for assessing differential expression in microarray experiments. Statistical Applications in Genetics and Molecular Biology. 2004; 3: Article3.

[12] Anders S, Huber W. Differential expression analysis for sequence count data. Genome Biology. 2010; 11: R106.

[13] Uhlén M, Björling E, Agaton C, Szigyarto CAK, Amini B, Andersen E, *et al*. A human protein atlas for normal and cancer tissues based on antibody proteomics. Molecular & Cellular Proteomics. 2005; 4: 1920–1932.

[14] Newman AM, Steen CB, Liu CL, Gentles AJ, Chaudhuri AA, Scherer F, *et al*. Determining cell type abundance and expression from bulk tissues with digital cytometry. Nature Biotechnology. 2019; 37: 773–782.

[15] Geeleher P, Cox N, Huang RS. pRRophetic: an R package for prediction of clinical chemotherapeutic response from tumor gene expression levels. PLoS ONE. 2014; 9: e107468.

[16] Rizzardi AE, Johnson AT, Vogel RI, Pambuccian SE, Henriksen J, Skubitz AP, *et al*. Quantitative comparison of immunohistochemical staining measured by digital image analysis versus pathologist visual scoring. Diagnostic Pathology. 2012; 7: 42.

[17] Trott O, Olson AJ. AutoDock Vina: improving the speed and accuracy of docking with a new scoring function, efficient optimization, and multithreading. Journal of Computational Chemistry. 2010; 31: 455–461.

Journal of
BIOLOGICAL REGULATORS
and Homeostatic Agents

[18] Salentin S, Schreiber S, Haupt VJ, Adasme MF, Schroeder M. PLIP: fully automated protein-ligand interaction profiler. Nucleic Acids Research. 2015; 43: W443–W447.

[19] Aashiq M, Silverman DA, Na'ara S, Takahashi H, Amit M. Radioiodine-Refractory Thyroid Cancer: Molecular Basis of Redifferentiation Therapies, Management, and Novel Therapies. Cancers. 2019; 11: 1382.

[20] Sun J, Li Y. Pyroptosis and respiratory diseases: A review of current knowledge. Frontiers in Immunology. 2022; 13: 920464.

[21] Liou AKF, Soon G, Tan L, Peng Y, Cher BM, Goh BC, *et al*. Elevated IL18 levels in Nasopharyngeal carcinoma induced PD-1 expression on NK cells in TILS leading to poor prognosis. Oral Oncology. 2020; 104: 104616.

[22] Li J, Qiu G, Fang B, Dai X, Cai J. Deficiency of IL-18 Aggravates Esophageal Carcinoma Through Inhibiting IFN-γ Production by $CD8^{+}$T Cells and NK Cells. Inflammation. 2018; 41: 667–676.

[23] Abdolahi F, Dabbaghmanesh MH, Haghshenas MR, Ghaderi A, Erfani N. A gene-disease association study of IL18 in thyroid cancer: genotype and haplotype analyses. Endocrine. 2015; 50: 698–707.

[24] Chung JH, Lee YC, Eun YG, Chung JH, Kim SK, Chon S, *et al*. Single Nucleotide Polymorphism of Interleukin-18 and Interleukin-18 Receptor and the Risk of Papillary Thyroid Cancer. Experimental and Clinical Endocrinology & Diabetes. 2015; 123: 598–603.

[25] Colp C, Goldfarb A, Wei I, Graney J. Patient's self-interpretation of tuberculin skin tests. Chest. 1996; 110: 1275–1277.

[26] Carneiro RM, Carneiro BA, Agulnik M, Kopp PA, Giles FJ. Targeted therapies in advanced differentiated thyroid cancer. Cancer Treatment Reviews. 2015; 41: 690–698.

[27] Capdevila J, Trigo JM, Aller J, Manzano JL, Adrián SG, Llopis CZ, *et al*. Axitinib treatment in advanced RAI-resistant differentiated thyroid cancer (DTC) and refractory medullary thyroid cancer (MTC). European Journal of Endocrinology. 2017; 177: 309–317.

[28] Gruber JJ, Colevas AD. Differentiated thyroid cancer: focus on emerging treatments for radioactive iodine-refractory patients. The Oncologist. 2015; 20: 113–126.